Femtosecond X-ray Pulses From a Frequency Chirped SASE FEL

S. Krinksy
National Synchrotron Light Source

And

Z. Huang
Stanford Linear Accelerator Center
Stanford, California 94309

September, 2003

DISCLAIMER

Femtosecond X-ray Pulses From a frequency chirped SASE FEL

Z. Huang[1]

Stanford Linear Accelerator Center, Stanford, CA 94309

S. Krinsky

Brookhaven National Laboratory, Upton, NY 11973

Abstract

We discuss the temporal and spectral properties of self-amplified spontaneous emission (SASE) utilizing an energy-chirped electron beam. A short temporal pulse is generated by using a monochromator to select a narrow radiation bandwidth from the frequency chirped SASE. For the filtered radiation, the minimum pulse length is limited by the intrinsic SASE bandwidth, while the number of modes and the energy fluctuation can be controlled through the monochromator bandwidth. Two cases are considered: (1) placing the monochromator at the end of a single long undulator; (2) placing the monochromator after an initial undulator and amplifying the short-duration output in a second undulator. We analyze these cases and show that tens of femtosecond x-ray pulses may be generated for the linac coherent light source.

Key words: Femtosecond X-ray, Frequency Chirped Self-Amplified Spontaneous Emission
PACS: 41.60.Cr, 42.25.Kb

1 Introduction

The generation of femtosecond x-ray pulses is critical to exploring the ultrafast science at an x-ray free-electron laser (FEL) facility based on self-amplified spontaneous emission (SASE) [1,2]. Since the pulse length of typical electron

---

[1] Corresponding author (Email: zrh@slac.stanford.edu)

bunches that drive the SASE FEL is on the order of 100 femtosecond, many schemes have been proposed to reduce the pulse length of x-ray pulses generated from the electron bunches that drive the SASE FEL [3–11]. Among them, a number of optical schemes are based on x-ray manipulations (such as compressing and slicing) of a frequency chirped SASE [3,4,7]. In this paper, we study the temporal and spectral properties of a frequency chirped SASE and show that the minimum x-ray pulse length in these optical schemes is determined by the SASE bandwidth and the amount of energy chirp allowed by the accelerator and the FEL performance. In particular, we consider two approaches that use a monochromator to control the radiation pulse for the linac coherent light source (LCLS) and discuss the expected pulse length, the energy fluctuation, and the number of x-ray photons.

2   Statistical Properties of a Frequency Chirped SASE

In this section, we briefly discuss the statistical properties of a frequency chirped SASE, based on the one-dimensional FEL analysis of Ref. [12]. Consider an energy-chirped electron bunch passing through a planar undulator having period $\lambda_w = 2\pi/k_w$ and rms undulator strength parameter a_w. The jth electron has energy γ_j (in units of its rest mass) and arrives at the undulator entrance at time t_j. Suppose that the electron energy chirp is linear and is specified by

$$\frac{\gamma_j - \gamma_0}{\gamma_0} = \alpha \frac{t_j}{T_b}, \tag{1}$$

where $\gamma_0 mc^2$ is the central energy of the electron bunch, and T_b is the full pulse length of a flat-top electron bunch. Due to the resonance condition, the

undulator radiation has a linear frequency chirp given by

$$\omega_j = k_j c = \frac{2\gamma_j^2 k_w c}{1 + a_w^2} \approx \omega_0 + u t_j \,, \tag{2}$$

where $u = 2\alpha\omega_0/T_b$, and $\omega_0 = k_0 c = 2\gamma_0^2 k_w c/(1 + a_w^2)$.

In the exponential growth regime before saturation, the electric field of the frequency chirped SASE at the undulator distance z is

$$E(z,t) \propto \sum_j e^{ik_j z - i\omega_j(t-t_j)} g(z, t - t_j, u) \,. \tag{3}$$

To the first order in u, the Green's function can be approximated by

$$g(z, t - t_j, u) \approx \exp\left[(\sqrt{3} + i)\rho k_w z - \frac{3}{4}\left(1 + \frac{i}{\sqrt{3}}\right)\sigma_\omega^2\left(t - t_j - \frac{z}{v_g}\right)^2 \right]$$
$$\times \exp\left[-\frac{iu}{2}\left(t - t_j - \frac{z}{v_0}\right)\left(t - t_j - \frac{z}{c}\right) \right] \,, \tag{4}$$

where ρ is the FEL scaling parameter [13], σ_ω is the SASE bandwidth [14,15],

$$\frac{\sigma_\omega}{\omega_0} = \left(\frac{3\sqrt{3}}{k_w z}\rho\right)^{1/2} \,, \tag{5}$$

$v_g = \frac{\omega_0}{(k_0 + 2k_w/3)}$ is the group velocity of the radiation wave packet, and $v_0 = \omega_0/(k_0 + k_w)$ is the average electron velocity. We note that in addition to the dependence of frequency on arrival time, $\omega_j \approx \omega_0 + u t_j$, the frequency chirp also appears in the Green's function since the gain process depends on the electrons within one radiation slippage length.

Equation (3) determines the temporal and the spectral properties of a frequency chirped SASE. Treating the arrival time t_j as a random variable, we can average over the stochastic ensemble to obtain the coherence time [16,17,12]

$$\tau_{\rm coh} = \int d\tau \left| \frac{\langle E(z, t - \tau/2) E^*(z, t + \tau/2)\rangle}{\langle |E(z,t)|^2\rangle} \right|^2 = \frac{\sqrt{\pi}}{\sigma_\omega} \,, \tag{6}$$

which is independent of the electron energy chirp. Fourier transforming Eq. (3),

we obtain the radiation field in frequency domain $\tilde{E}(z, \omega)$. The range of spectral coherence is given by [12]

$$\Omega_{\text{coh}} = \int d\tau \left| \frac{\langle E(z, \omega - \Omega/2) E^*(z, \omega + \Omega/2) \rangle}{\langle |E(z, \omega)|^2 \rangle} \right|^2 = |u| \frac{\sqrt{\pi}}{\sigma_\omega} = |u| \tau_{\text{coh}}, \qquad (7)$$

where we have assumed $u\tau_{\text{coh}} \gg 2\pi/T_b$ for a long electron pulse. Because of the noisy start-up, the frequency chirped SASE is organized into M independent longitudinal modes in both time and frequency domains, where

$$M = \frac{T_b}{\tau_{\text{coh}}} = \frac{|u| T_b}{\Omega_{\text{coh}}}. \qquad (8)$$

The relative radiation energy fluctuation is given by $M^{-1/2}$.

3   Short X-ray Pulse Generation

A monochromator can be used to select a short portion of the frequency chirped SASE pulse. Let us assume the monochromator is centered at ω_m with an rms bandwidth σ_m, the filtered electric field after the monochrmator is

$$E_F(z, t) = \int \frac{d\omega}{2\pi} e^{-i\omega t} \tilde{E}(z, \omega) \exp \left[-\frac{(\omega - \omega_m)^2}{4\sigma_m^2} \right], \qquad (9)$$

The intensity of the sliced x-ray pulse can be computed as [12]

$$I_F \propto \langle |E_F(z, t)|^2 \rangle \propto e^{2\sqrt{3}\rho k_w z} \exp \left[-\frac{t - t_m)^2}{2\sigma_t^2} \right], \qquad (10)$$

where the pulse arrival time is

$$t_m(z) = \frac{\omega_m - \omega_0}{u} + \frac{1}{2} \left(\frac{z}{v_0} + \frac{z}{c} \right), \qquad (11)$$

and the rms pulse duration σ_t is given by

$$\sigma_t^2(z) = \frac{\sigma_\omega^2(z) + \sigma_m^2}{u^2} + \frac{1}{4\sigma_m^2}. \qquad (12)$$

4

Equation (12) shows that the pulse duration cannot be made smaller than σ_ω/u, as illustrated in the phase space geometry of Fig. 1. This limitation to the attainable pulse length is applicable to both pulse slicing and compression. Another limitation of these optical schemes is the bandwidth of optical elements. In the case of a monochromator, an extremely narrow bandwidth will stretch the pulse due to Fourier transform limit, as expressed by the last term in Eq. (12). The optimal monochromator bandwidth that yields the minimum pulse duration is

$$\frac{(\sigma_m)_{\text{opt}}}{\omega_0} = \sqrt{\frac{|u|}{2\omega_0^2}}. \tag{13}$$

The corresponding minimum rms pulse duration is

$$(\sigma_t)_{\text{min}} = \sqrt{\frac{\sigma_\omega^2 + |u|}{u^2}}. \tag{14}$$

In principle, for a given SASE bandwidth, one can increase the energy chirp α and hence the frequency chirp u to select a shorter pulse. The maximum chirp without significantly degrading the FEL gain is $u \sim \sigma_\omega^2$ [7]. From Eq. (14), we see that $(\sigma_t)_{\text{min}} \sim \sqrt{2}/\sigma_\omega \sim \tau_{\text{coh}}$, i.e., a single coherent spike may be selected. However, as shown in the following section, the required energy chirp for a single spike selection is typically too large for the normal accelerator operations.

Finally, the fractional shot-to-shot energy fluctuation σ_W/W after the monochromator can be expressed as [12]

$$\frac{\sigma_W^2}{W^2} = \frac{|u|}{\sqrt{u^2 + 4\sigma_m^2\sigma_\omega^2}} \equiv \frac{1}{M_F}, \tag{15}$$

where

$$M_F = \sqrt{\frac{4\sigma_m^2\sigma_\omega^2}{u^2} + 1} \approx \frac{2\sigma_m}{|u|/\sigma_\omega} = \frac{2\sqrt{\pi}\sigma_m}{\Omega_{\text{coh}}}, \tag{16}$$

when $2\sqrt{\pi}\sigma_m \gg \Omega_{\text{coh}}$. Thus, M_F is the number of spectral modes that pass the monochromator with a "full" bandwidth $2\sqrt{\pi}\sigma_m$. The coherence time of

the filtered radiation can be calculated similar to Eq. (6) as

$$(\tau_{\mathrm{coh}})_F = \frac{2\sqrt{\pi}\sigma_t}{M_F}. \tag{17}$$

4   Application to the LCLS

We now apply these results to pulse slicing schemes proposed for the LCLS operated at the fundamental wavelength 1.5 Å (i.e., $\omega_0 = 1.2 \times 10^{19}$ s^{-1}) [1]. The norminal LCLS design has a nearly flat-top electron bunch with a FWHM duration $T_b = 230$ fs. Since the SASE intrinsic bandwidth is an important limiting factor to the attainable x-ray pulse length, we use the time-dependent FEL simulation code GINGER [18] to determine it along the LCLS undulator. Figure 2 shows the normalized rms bandwidth $\sigma_\omega/(\rho\omega_0)$ and the power in the normal SASE operations of the LCLS. Near saturation, the minimum rms bandwidth is $(\sigma_\omega)_{\min} \approx \rho = 5 \times 10^{-4}$, as expected from the 1D formula (i.e., Eq. (5)). However, in the early exponential growth regime, the SASE bandwidth is substantially larger than the 1D prediction ($\propto z^{-1/2}$) due to the existence of higher-order transverse modes. Note that the coherence time near saturation is $\tau_{\mathrm{coh}} = \sqrt{\pi}/(\sigma_\omega)_{\min} \approx 0.3$ fs and the number of longitudinal modes is $M \approx 766$.

The maximum allowable chirp without significantly degrading the FEL gain is $u \sim \sigma_\omega^2$, corresponding to a linear energy chirp $\alpha \sim 35\%$, which is obviously too large for the normal acceleration operations. Tracking studies suggest that a maximum energy chirp of 2% across the whole bunch is possible for the LCLS accelerator, although a 1% energy chirp is more accessible [1]. Thus, we take $\alpha = 0.01$, $u = 7 \times 10^{-9}\omega_0^2 \ll \sigma_\omega^2$ and consider two cases: (1) placing the monochromator at the end of a single long undulator in the one-

6

stage approach; (2) placing the monochromator after an initial undulator and amplifying the short-duration output in a second undulator in the two-stage approach.

4.1 One-stage Approach

In the one-stage approach, the monochromator is place at the end of the undulator where the frequency chirped SASE reaches power saturation [3]. At this point, the SASE bandwidth also reaches the minimum. We can further minimize the sliced pulse length by choosing the optimal monochromator bandwidth given by Eq. (13), i.e.,

$$\frac{(\sigma_m)_{\mathrm{opt}}}{\omega_0} = \sqrt{\frac{|u|}{2\omega_0^2}} = 6 \times 10^{-5} .$$ (18)

Since $|u| \ll \sigma_\omega^2$, the minimum rms pulse duration from Eq. (14) is

$$(\sigma_t)_{\mathrm{min}} \approx \frac{(\sigma_\omega)_{\mathrm{min}}}{u} = 6 \text{ fs} ,$$ (19)

and the minimum fwhm pulse duration is about 15 fs. At this minimum, the number of longitudinal modes is $M_F \approx 2\sigma_m \sigma_\omega / u = 9$, corresponding to a fractional energy fluctuation $M_F^{-1/2} = 33\%$.

In Fig. 3, we plot the sliced rms pulse duration σ_t and the number of modes M_F as a function of the monochromator bandwidth, given by Eqs. (12) and (16), respectively. The minimum of σ_t is broad as it is dominated by the relatively large SASE bandwidth. Since M_F depends nearly linearly on the monochromator bandwidth, one can change σ_m over the range $(\sigma_m)_{\mathrm{opt}} < \sigma_m < \sigma_\omega$ to reduce the energy fluctuation with little increase in the pulse duration. For instance, at a much larger monochromator bandwidth $\sigma_m = 4 \times 10^{-4}$, Fig. 3 shows that the rms pulse duration is slightly increased to 7.5 fs, but

the fractional energy fluctuation can be reduced to $1/\sqrt{60} \approx 13\%$. Since the number of x-ray photons passing through the monochromator is proportional to $\sigma_m \sigma_t \approx \sigma_m \sigma_\omega / u$ near the minimum pulse duration, a larger monochromator bandwidth also increases the available x-ray photons for the experimental stations.

4.2 Two-stage Approach

In the two-stage approach, the monochromotor is placed after the first undulator to select a short pulse from a frequency chirped SASE in the exponential growth regime. The short duration radiation is then amplified to saturation in the second undulator by the same energy-chirped electron bunch [7]. Since the peak power after the first undulator is much less than the saturation power, the damage to optical elements of the monochromator is reduced. However, the SASE bandwidth is also larger than the minimum bandwidth at saturation. For example, Fig. 2 shows that the relative rms SASE bandwidth is about $2\rho = 1 \times 10^{-3}$ at $z = 50$ m in the LCLS undulator, twice as large as the minimum bandwidth near saturation. From the analysis of previous sections, we see that the minimum rms pulse duration sliced at this undulator location is 12 fs (30 fs fwhw), two times larger than that given in Eq. (19). After its microbunching is destroyed in a bypass chicane, the chirped electron bunch is brought into the second undulator to amplify the short radiation pulse until it reaches the full saturation power. Note that for effective FEL interaction in the second undulator, the radiation pulse after the monochromator should overlap with the resonant part of the chirped electron bunch having the appropriate energy. Thus, the relative time delay between the optical and electron paths at the entrance of the second undulator can not be much longer than

8

10 fs.

5 Conclusions

In this paper, we present the statistical properties of a frequency chirped SASE FEL, which form the basis for any optical manipulation of such a radiation pulse. We apply this analysis to the pulse slicing schemes using a monochromator and determine the minimum pulse duration, the number of modes and the energy fluctuation. Two pulse slicing configurations for the LCLS are discussed. In the one-stage approach, a shortest x-ray pulse ($\sim$ 10 fs) can be selected at the FEL saturation because the SASE bandwidth reaches the minimum. Increasing the monochromator bandwidth just below the SASE bandwidth only slightly lengthens the selected pulse, but significantly reduces the energy fluctuation and increases the x-ray photons for experiments. In the two-stage approach, the selected pulse is somewhat longer than that obtained from the one-stage approach because the slicing occurs at a larger SASE bandwidth before saturation, but it can be amplified in the second undulator to reach the same peak power as a saturated FEL.

6 Acknowledgments

References

[1] Linac Coherent Light Source Conceptual Design Report, SLAC-R-593, 2002.

[2] TESLA Techinical Design Report, DESY TESLA-FEL 2001-05, 2001.

[3] V. Bharadwaj *et al.*, LCLS-TN-00-8, 2000.

[4] C. Pellegrini, Nucl. Instrum. Meth. A **445**, 124 (2000).

[5] W. Brefeld *et al.*, DESY 01-063, 2001.

[6] W. Brefeld *et al.*, Nucl. Instrum. Meth. A **483**, 75 (2002).

[7] C.B. Schroeder *et al.*, Nucl. Instrum. Meth. A **483**, 89 (2002); J. Opt. Soc. Am. B **19** (2002).

[8] E.L. Saldin, E.A. Schneidmiller, M.V. Yurkov, Opt. Commun. **212**, 377 (2002).

[9] S. Reiche, P. Emma, C. Pellegrini, Nucl. Instrum. Meth. A **507**, 426 (2003)

[10] P. Emma and Z. Huang, in these proceedings, 2003.

[11] P. Emma *et al.*, SLAC-PUB-10002, submitted to Phys. Rev. Lett., 2003.

[12] S. Krinsky and Z. Huang, Phys. Rev. ST Accel. Beams **6**, 050702 (2003).

[13] R. Bonifacio, C. Pellegrini, and L.M. Narducci, Opt. Commun. **50**, 373 (1984).

[14] K.-J. Kim, Nucl. Instrum. Meth. A **250**, 396 (1986).

[15] J.-M. Wang and L.-H. Yu, Nucl. Instrum. Meth. A **250**, 484 (1986).

[16] J.W. Goodman, *Statistical Optics*, (John Wiley & Sons, New York, 1985).

[17] E.L. Saldin, E.A. Schneidmiller and M.V. Yurkov, *The Physics of Free Electron Lasers*, (Springer, Berlin, 2000).
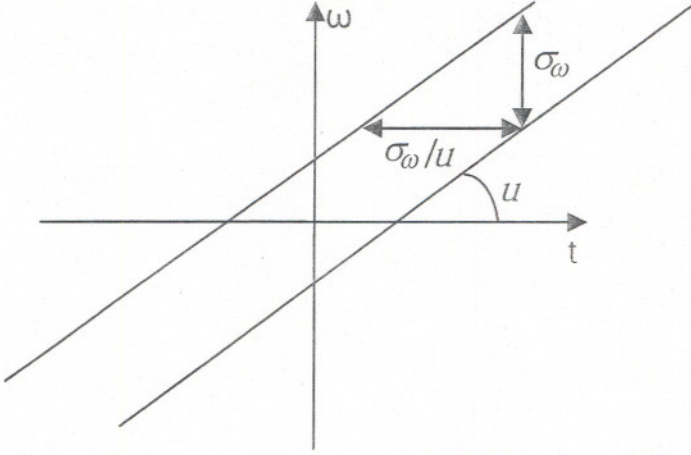
[18] W. Fawley, Report LBNL-49625, 2002.

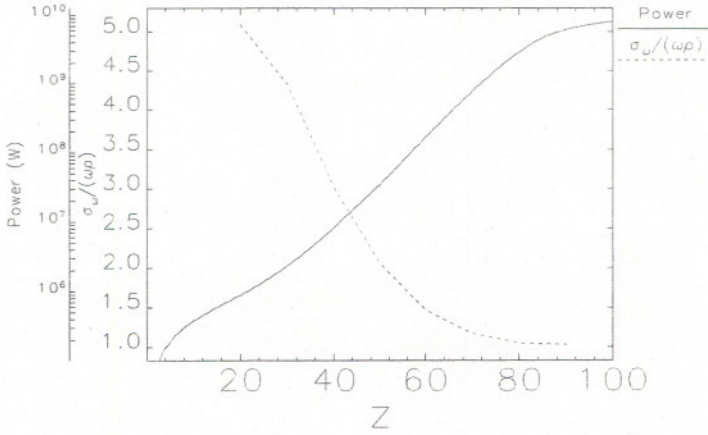Fig. 1. Longitudinal phase space of a frequency chirped SASE.

Fig. 2. GINGER simulation of SASE power (solid) and bandwidth (dashed) as a function of the undulator distance z in the LCLS undulator.
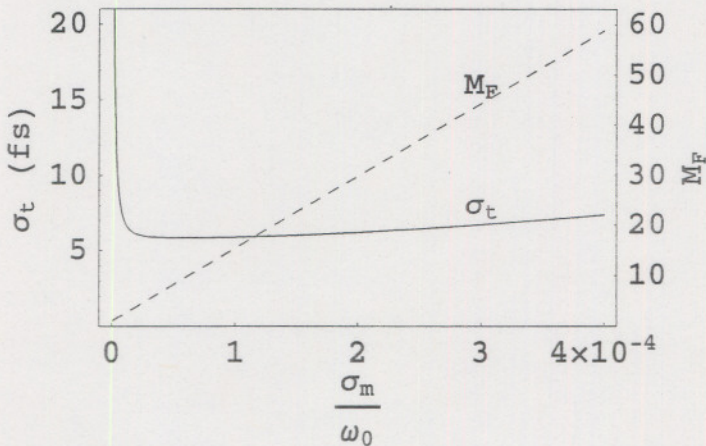
Fig. 3. RMS pulse duration σ_t (solid) and the number of modes M_F (dashed) as a function of the rms bandwidth σ_m of the monochromator placed at the end of the LCLS undulator ($\sigma_\omega/\omega \approx \rho = 5 \times 10^{-4}$) for a (full) energy chirp of 1%.